ELSEVIER

International Journal of Mass Spectrometry 181 (1998) 181–199

International Journal of Mass Spectrometry

The measurement of high proton affinities for a variety of metallic compounds: a new approach by flame-ion mass spectrometry

QingFeng Chen, John M. Goodings*

Department of Chemistry, York University, 4700 Keele Street, Toronto, Ontario M3J 1P3, Canada

Received 15 July 1998; accepted 6 October 1998

Abstract

A small amount ($\leq 10^{-6}$ mol fraction) of four alkaline earth metals, tin and yttrium were introduced into five, premixed, fuel-rich, H_2–O_2–N_2 flames at atmospheric pressure in the temperature range 1820–2400 K. Aqueous salt solutions of the metals were sprayed into the premixed flame gas as an aerosol using an atomizer technique. Ions in a flame were observed by sampling flame gas through a nozzle into a mass spectrometer. The concentrations of the major neutral metallic species present in the flame were calculated from thermodynamic data currently available. The principal metallic ions observed were AOH^+ (A = Mg, Ca, Sr, Ba, Sn) and $A(OH)_2^+$ (A = Y), formed initially by proton transfer to AO and OAOH from H_3O^+, a natural flame ion. Except for Mg, the ions were also produced by chemi-ionization processes. By adjusting the concentration(s) of the salt solution in the atomizer, it was found that a pair of ions could be brought into equilibrium within the time scale of the flame; the pairs included H_3O^+ with a metal ion or two metallic ions. Because water is a major product of combustion, a very large difference in proton affinity $PA^0(AO) - PA^0(H_2O) \leq 490$ kJ mol^{-1} (117 kcal mol^{-1}) could be attempted for the proton transfer equilibrium. Using $PA^0(H_2O) = 691.0$ kJ mol^{-1} (165.2 kcal mol^{-1}) as a reference base to anchor the proton affinity scale, ion ratio measurements led to proton affinity PA^0 values of 766, 912, 1004, 1184, 1201, and 1222 kJ mol^{-1} (183, 218, 240, 283, 287, and 292 kcal mol^{-1}) corrected to 298 K for OYOH, SnO, MgO, CaO, SrO, and BaO, respectively; of these, only the value for OYOH has not been reported previously. If it is assumed that the neutral thermodynamic data are correct (although some appear to be in error), the uncertainties in the PA results reported here are ± 21 kJ mol^{-1} (5 kcal mol^{-1}). The realization that these equilibria can be achieved in flames provides a new approach to consolidate and build the high end of the proton affinity ladder, primarily of metallic species which are not accessible at lower temperatures. (Int J Mass Spectrom 181 (1998) 181–199) © 1998 Elsevier Science B.V.

Keywords: Proton affinity; Metallic compounds; Flames; Flame ionization; Mass spectrometry

1. Introduction

A large number of proton affinities (PA) of atoms and molecules have been measured in the gas phase. A compilation is available on the internet at the NIST Chemistry WebBook site [1] as an outgrowth of the earlier tables by Lias et al. [2]. In general, the PAs for different types of compounds are accessible in different temperature ranges using a variety of measurement techniques. A great many PAs of organic molecules have been determined near room temperature

* Corresponding author. E-mail: goodings@turing.sci.yorku.ca

PII S1387-3806(98)14201-X

with ion cyclotron resonance (ICR) spectrometers and flowing afterglow methods (FA; e.g. selected ion flow tube, SIFT). Recently, two versions of a high-temperature flowing afterglow apparatus have been described, one of stainless steel construction for the range 300–1300 K and also a ceramic one covering 300–1600 K [3]. High pressure mass spectrometry (HPMS) has been employed in the range 300–900 K for organic compounds, but also by Kebarle and his co-workers [4,5] for protonated alkali metal hydroxides AOH_2^+ where $PA^0(AOH)$ is derived from the hydration energy of the equivalent $A^+ . H_2O$ ion. At higher temperatures in the approximate range 1500–2000 K, Murad used a Knudsen cell coupled to a mass spectrometer to measure appearance potentials of gaseous metallic ions from which the PAs of FeO [6], MgO, CaO, SrO, and BaO [7,8] can be derived. Inevitably, the associated errors are rather large because appearance potentials are typically measured to ± 0.2 eV (± 19 kJ mol^{-1} or ± 4.6 kcal mol^{-1}). Discrepancies are apparent in some of these data. Murad's values for $PA^0(AO)$ listed in the NIST compilation [1] show an increasing trend for Ca, Sr, and Ba, whereas the opposite trend is obtained from standard heats of formation for AO and AOH^+ given in the JANAF Tables [9].

Even higher temperatures in the range 1800–2600 K are available when a flame is used as an ion source for a flame-ion mass spectrometer (FIMS). A recent example is the measurement of $PA^0(CuOH)$ from the hydration energy for $Cu^+ . H_2O$ by Butler and Hayhurst [10]. Earlier, Jensen [11] measured $\Delta H_f^0(SnOH^+)$ from which $PA^0(SnO)$ can be obtained using additional data [12]. It is noteworthy, although perhaps not surprising, that the PAs of metallic compounds, primarily oxides and possibly hydroxides also, occur at the high end of the proton affinity ladder above about 840 kJ mol^{-1} (~ 200 kcal mol^{-1}).

The present work involves a new approach to study the high end of the proton affinity ladder involving metallic compounds in flames. When a pair of metals is introduced into a series of flames in the temperature range 1820–2400 K, in most cases the metals will ionize to some extent. The metallic ions can usually be brought into chemical equilibrium within the time scale of a flame's burnt-gas region by judicious adjustment of the concentrations. If K_{eq} is the equilibrium constant of an equilibrated proton transfer reaction, the slope of a van't Hoff plot of ln K_{eq} versus inverse temperature yields the difference in PA of the two metallic neutral species. The measurement involves only an ion signal ratio, not absolute ion concentrations. However, the composition of the metallic neutrals must be known at the flame temperatures. Results are presented for a number of pairs of metals which include the alkaline earths, tin and yttrium. In a few cases, a metallic ion can be equilibrated with H_3O^+, a natural flame ion, to anchor the PA ladder to $PA^0(H_2O)$ = 691.0 kJ mol^{-1} (165.2 kcal mol^{-1}) [1].

2. Experiment

Five, premixed, laminar, flat, H_2–O_2–N_2 flames at atmospheric pressure of fuel-rich composition (equivalence ratio ϕ = 1.5) in the temperature range 1820–2400 K were employed for this work. Their properties including the calculated compositions of the equilibrium burnt gas based on the JANAF Tables [9] are listed in Table 1. The concentrations of free radicals overshoot their equilibrium values in the reaction zone of each flame and then decay downstream towards equilibrium in the burnt gas; the effect is greater the cooler the flame. The degree of overshoot is specified by Sugden's disequilibrium parameter γ [13] defined as the ratio of the actual concentration of a species at any point in the flame to its equilibrium concentration in the burnt gas. For fuel-rich flames, where $[H_2O]$ and $[H_2]$ are constant in the burnt gas, $\gamma_H = \gamma_{OH} \equiv \gamma$ whereas $\gamma_O = \gamma^2$. For the five flames in Table 1, Butler and Hayhurst [10] have measured γ as a function of distance z along the flame axis. Even at z = 30 mm downstream in flames 3, 4, and 5, $\gamma \neq 1$. All five fuel-rich flames are cylindrical in shape with plug flow. They have a diameter of about 12 mm, and are stabilized on a water-cooled brass burner previously described [14].

Metals were introduced into the flames by spraying an aqueous solution into the premixed flame gas as an

Table 1
Properties of the hydrogen-oxygen-nitrogen flames

Flame number/property	2	25	3	4	5
Equivalence ratio ϕ	1.5	1.5	1.5	1.5	1.5
$H_2/O_2/N_2$	2.74/1/2.95	3.0/1/3.5	3.18/1/4.07	3.09/1/4.74	1.5/1/3.55
Total unburnt gas flow ($cm^3\ s^{-1}$)	300	250	250	200	150
Measured flame temperature (K)	2400	2230	2080	1980	1820
Rise velocity in burnt gas ($m\ s^{-1}$)	19.8	18.6	15.6	11.4	8.4
Equilibrium burnt gas composition (mole fractions)					
H_2O	0.3460	0.3063	0.2754	0.2553	0.2249
H_2	0.1286	0.1527	0.1622	0.1390	0.1259
O_2	0.000 105 7	0.000 007 90	0.000 000 72	0.000 000 18	0.000 000 01
H	0.006 019	0.002 650	0.001 077	0.000 500 8	0.000 141 5
OH	0.003 084	0.000 795 1	0.000 213 0	0.000 088 90	0.000 017 54
O	0.000 094 69	0.000 009 35	0.000 000 99	0.000 000 23	0.000 000 01
N_2	0.5157	0.5375	0.5610	0.6052	0.6490

aerosol derived from an atomizer described previously [15], operated by a flow of 16.2 $cm^3\ s^{-1}$ of the diluent nitrogen gas. Spraying a 0.1 M solution introduced 9.5×10^{-7} mol fraction of total metal into a premixed flow of 250 $cm^3\ s^{-1}$. The atomizer calibration departs from linearity when the total solution concentration exceeds approximately 0.15 M. A solution of two metallic salts provides a known concentration ratio of the metals in a flame. A convenient way to change the concentration ratio in the mixed solution was to set up two burettes, each one containing a fairly concentrated solution of a metallic salt. Aliquots drawn from each diluted with distilled water provided a wide range of concentrations and their ratios. The salts used to make up the solutions were acetates or chlorides of stated purity: $MgAc_2.4H_2O$ (> 98%) or $MgCl_2.6H_2O$ (99.99%); $CaAc_2.H_2O$ (Fisher Certified); $SrAc_2.\frac{1}{2}H_2O$ (> 98%); $BaCl_2.2H_2O$ (> 99%); $SnCl_4.5H_2O$ (> 98%); and $YCl_3.6H_2O$ (99.9%). Some of these salts contain traces of potassium yielding a relatively large and undesirable K^+ signal in the ion spectrum; e.g. for magnesium, K^+ from the high-purity chloride was much higher than the signal from the acetate of much lower purity so that the latter was employed.

The burner is mounted horizontally on a motorized carriage with calibrated drive coupled to the X axis of an XY recorder. The flame axis z is accurately aligned with the sampling nozzle of the mass spectrometer. Two types of conical sampling nozzles [14] were employed in these studies: those having a tiny electron microscope lens of Pt/Ir alloy swaged into the tip of a stainless steel cone, with orifice diameters of 0.104, 0.170, and 0.202 mm; and one in the form of a 60°, sharp-edged, electroformed, nickel cone with an orifice diameter of 0.181 mm at the tip. The latter type have a smaller thermal boundary layer such that the formation of ion hydrates as a result of cooling during sampling is minimized. This consideration can be important when two metals are sprayed if the mass numbers of their parent and hydrate ion signals overlap. The whole apparatus including the mass spectrometer has already been described in detail [14] so that only a brief outline will be given here. Flame gas including ions is sampled into a first vacuum chamber maintained at 0.04 Pa (3×10^{-4} Torr). The ions are formed into a beam by an electrostatic lens, pass through a 3 mm orifice in a nose cone into a second vacuum chamber maintained below 0.003 Pa ($< 2 \times 10^{-5}$ Torr), are conditioned by a second ion lens for analysis by a quadrupole mass filter, collected by a parallel-plate Faraday detector, and measured by a sensitive electrometer coupled to the Y axis of the XY recorder. Ion signal magnitudes measured in the figures below as a voltage (in mV) refer to the collected ion current passing through a grid-leak resistor of $10^{10}\ \Omega$. By driving a flame towards the sampling nozzle, the profile of an individual ion

signal versus distance along the flame axis z can be obtained. Experimentally, $z = 0$ is defined where the pressure abruptly rises when the sampling nozzle pokes through the flame reaction zone into the cooler unburnt gas upstream. The pressure is measured with an ionization gauge mounted on the second vacuum chamber. As an alternative to individual ions, total positive ion (TPI) profiles can be measured by switching off the dc voltages to the quadrupole rods. Still with the dc voltages switched off and the spectrometer's mass dial set to a given mass number, all of the ions above that mass are collected; e.g. TPI_{12} designates all of the positive ions (because no measurable flame ion signal exists below 12 u).

3. Comparison of experimental methods

In recent years, extensive experimental efforts [2,16] have been directed towards obtaining scales of proton affinities PA and gas-phase basicities GB, i.e. the enthalpy ΔH^0 and free energy ΔG^0 changes, respectively, for reactions

$$XH^+ \rightleftarrows X + H^+ \quad (1)$$

where X is a base compound, i.e. a proton acceptor. Generally speaking, there are five principal experimental methods mentioned in the introduction including FA (SIFT), HPMS, FIMS, ICR, and Knudsen cell mass spectrometry (KCMS) for obtaining the quantitative data required for setting up such PA scales. The first three methods involve measuring the equilibrium constant K_{eq} for proton transfer reactions of the type

$$XH^+ + B \rightleftarrows X + BH^+ \quad (2)$$

$$K_{eq} = [X][BH^+]/[B][XH^+] \quad (3)$$

where isotopic corrections must be made if only the principal isotope is measured.

For the conventional FA and SIFT experiments, K_{eq} is measured at a single temperature T leading to the usual expression for $\Delta G^0 = -\ RT\ \ln K_{eq} = \Delta H^0 - T\Delta S^0$. The enthalpy changes required for the PA scales can then be obtained from ΔG^0 values by estimating a value for ΔS^0. The method has the disadvantage that ΔS^0 is not always easy to estimate. For temperature-variable FA, HPMS, and FIMS, K_{eq} is measured at a series of temperatures. A linear van't Hoff plot of $\ln K_{eq}$ against $1/T$ from $\ln K_{eq} = -\Delta H^0/RT + \Delta S^0/R$ then directly yields ΔH^0 from the slope and ΔS^0 from the intercept under the assumptions that ΔH^0 and ΔS^0 are constant over the experimental temperature range (second law treatment). These three methods have major advantages for minimizing errors because random errors in K_{eq} and T will tend to cancel in a linear fit to the data, and ΔS^0 need no longer be estimated. However, systematic errors in K_{eq} may still arise. For example, if the two ion signals XH^+ and BH^+ are subject to mass discrimination, an incorrect value $K'_{eq} = K_{eq} \times f$ is obtained, where f is a constant factor which is independent of temperature. The slope of the van't Hoff plot will still give the correct value of ΔH^0 although the intercept will be $\Delta S^0/R + \ln f$. The above equilibrium measurements only yield relative values of PA because $\Delta H^0_2 = PA^0(X) - PA^0(B)$. To assign an absolute PA value for B, it must be anchored to X, a standard reference base whose value is known.

For certain species where equilibrium constants of proton transfer reactions are difficult or impossible to measure, ICR methods may be used to estimate PA values [17]. In this approach, XH^+ is reacted with a series of bases. If the PA of X lies between those of bases B_1 and B_2, reaction (2) occurs for B_1 but not for B_2. Such a "bracketing" technique is less reliable than other methods because numerous complications can arise [2].

Another method which does not involve measuring K_{eq} for proton transfer reactions is KCMS [6–8]. In this approach, the dissociation energy $D^0(X - H)$ and the ionization energy $IE^0(XH)$ of XH are measured mass spectrometrically by passing hydrogen over ultra-pure X in a Knudsen cell. Then $PA^0(X) = D^0(X - H^+)$ can be derived from the measurements. In these studies, X was generally a metallic oxide AO. One advantage of KCMS, and of ICR also, is that the neutral concentrations of X and/or B need not be known.

At low temperatures, conventional FA, SIFT, ICR,

and HPMS methods are mainly suitable for organic compounds which cover the low end of the PA ladder. For metallic compounds which do not decompose at high temperatures, KCMS and FIMS are preferred techniques although the PA values measured at cell and flame temperatures have to be corrected to 298 K. Organic compounds will break up or decompose at the operating temperatures of Knudsen cells and flames.

Compared to other methods, FIMS has some distinct advantages for the study of metallic compounds which occupy the high end of the PA ladder. In the results reported here, one important feature is that K_{eq} has been measured in five flames over a temperature range spanning nearly 600 K, larger than that of the usual HPMS experiments ($<$ 300 K). Also, the requirement for high sample purity is less stringent than for KCMS. Using the atomizer technique, virtually any metal can be introduced into the flame for which an aqueous salt solution can be prepared. Water, which is a major product of the flame's combustion reaction, can often act as the anchoring reference base. The major drawback of FIMS is that the neutral concentrations [X] and [B] must be known, e.g. they are often calculated from data available in the JANAF Tables [9]. The neutral concentrations are not measured by the FIMS experiment because the flame is the only ion source. In some cases, there are significant discrepancies amongst different thermodynamic values in the literature. Obviously, the present results will be affected if the thermodynamic data, e.g. in the JANAF Tables [9], are wrong.

4. Composition of metallic neutral species in flames

The alkaline earth metals Mg, Ca, Sr, and Ba may be present in these flames as the neutral species A, AO, AOH, and $A(OH)_2$. For tin Sn, the major species are A and AO, whereas for yttrium Y they are AO and OAOH. When a sample from the atomizer is introduced into the flame, initially all of the metal is present as atomic A; then, the monohydroxide may form by the fast balanced reaction (denoted by = sign)

$$A + H_2O = AOH + H \quad (4)$$

Additional fast balanced reactions can then produce the dihydroxide and also the oxide

$$AOH + H_2O = A(OH)_2 + H \quad (5)$$

$$A + H_2O = AO + H_2 \quad (6)$$

For yttrium, where the oxide–hydroxide as well as the oxide is present

$$AO + H_2O = OAOH + H \quad (7)$$

The relative equilibrium concentrations of the neutral metallic species have been calculated using data from the JANAF Tables [9], and are given in Table 2 for all five flames; the metallic ions constitute only a negligible fraction of the total metal present. Because reactions (4), (5), and (7) involve the radical H, the relative concentrations of the metallic species depend on the disequilibrium parameter γ and vary in the burnt gas wherever γ varies; equations for the γ dependence have been given by Hayhurst and Kittelson [18]. As an example, calculated profiles of the four barium neutral species along the axis of flame 2 are given in Fig. 1. It has been assumed that all of the barium is initially present upstream as atomic Ba after dissociation of the chloride salt early in the reaction zone. For this flame at 2400 K, γ decreases and reaches unity at $z \approx 7$ mm downstream. Further downstream, the four neutral concentrations maintain their constant equilibrium values. In contrast, similar plots for the four neutral species in flames at lower temperatures (3–5, not shown) do not achieve their constant equilibrium values within the first 30 mm of the burnt gas because γ continues to decay throughout the whole region.

The enthalpies of formation of some metallic neutral compounds have been determined by a number of authors [9]. However, various mass-spectrometric and optical techniques employed such as flame ionization, crossed-beam reaction methods, laser-induced fluorescence, flame spectrophotometry, etc.

Table 2
Percentage of metallic compounds at equilibrium in all five flames ($\gamma = 1$)[a]

Element/%	[A]	[AO]	[A(OH)]	[$A(OH)_2$]	[OAOH]
Flame 2					
Ba	0.087	29.302	6.461	64.150	···
Sr	1.752	1.323	20.163	76.762	···
Ca	1.649	0.127	16.723	81.501	···
Mg	61.618	1.388	20.076	16.918	···
Sn	2.854	97.146	0	0	···
Y	···	16.86	···	···	83.14
Flame 25					
Ba	0.049	15.341	5.599	79.011	···
Sr	1.053	0.434	15.855	82.658	···
Ca	0.881	0.031	11.796	87.292	···
Mg	56.259	0.473	19.315	23.953	···
Sn	3.131	96.869	0	0	···
Y	···	10.84	···	···	89.16
Flame 3					
Ba	0.021	6.903	4.033	89.043	···
Sr	0.520	0.133	11.224	88.123	···
Ca	0.384	0.007	7.443	92.166	···
Mg	45.609	0.161	18.016	36.214	···
Sn	3.037	96.963	0	0	···
Y	···	9.07	···	···	90.93
Flame 4					
Ba	0.009	3.687	2.748	93.556	···
Sr	0.251	0.055	7.806	91.888	···
Ca	0.168	0.002	4.734	95.096	···
Mg	33.075	0.075	15.977	50.873	···
Sn	2.440	97.560	0	0	···
Y	···	7.15	···	···	92.85
Flame 5					
Ba	0.001	0.669	0.467	98.863	···
Sr	0.080	0.012	4.344	95.564	···
Ca	0.045	3×10^{-4}	2.253	97.702	···
Mg	17.543	0.015	10.877	71.565	···
Sn	1.940	98.060	0	0	···
Y	···	4.0	···	···	96.0

[a] The concentration data for Sn and Y are less accurately known than those for the alkaline earth metals listed in the JANAF Tables [9].

yield conflicting results. There are significant discrepancies in the neutral thermodynamic data taken from different literature sources, even for diatomic molecules [9,19–21]. They will affect the present results because a large uncertainty must be included to encompass the range of measured values. A comparison of data available for the alkaline earth metals is given in Table 3. The discrepancies for MgO and MgOH are particularly large. We have recently studied magnesium in some detail, both theoretically and experimentally, and the results will be presented in a later paper to follow very soon [22]. High-level ab initio calculations resulting in standard enthalpies of formation were carried out for eight magnesium species including ions. Our recommended values include $\Delta H^0_{f,298}(\mathrm{MgO}) = 149.4 \pm 12.6$ and $\Delta H^0_{f,298}(\mathrm{MgOH}) = -106.3 \pm 12.6$ kJ mol^{-1}. They are in best agreement with the values by Operti et al. [20] of 150.6 ± 20.9 for MgO and -92.1 ± 33.5 kJ mol^{-1} for MgOH. The use of our recommended values would considerably change the neutral composition of the magnesium species in the flames. Because the justification of these new data has not been published, only values from the JANAF Tables [9] have been

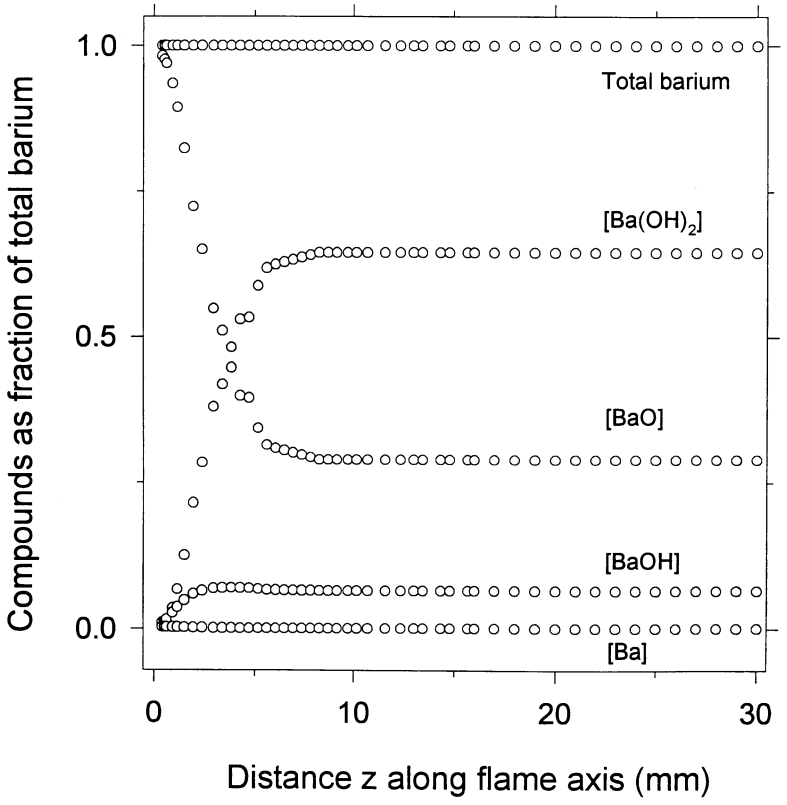

Fig. 1. Profiles of barium neutral compounds along the axis z of flame 2 at 2400 K. The flame reaction zone is located near $z = 0$ mm.

employed in this article. However, this example emphasizes the fact that, although FIMS can be an important method for obtaining PA values, the values depend strongly on the accuracy of the thermodynamic data available for metallic neutral compounds.

Table 3
Neutral standard enthalpies of formation at 298 K for alkaline earth metal compounds[a]

Compound	$\Delta H^0_{f,298}$ (kJ mol^{-1})
MgO	58.2 ± 25.1 [9]; 56.1 [19]; 150.6 ± 20.9 [20]
CaO	43.9 ± 21.0 [9]; 27 ± 17 [19]
SrO	− 13.4 ± 16.7 [9,19]; 1.5 ± 15 [21]
BaO	− 123.8 ± 8.0 [9,19]; − 112 ± 5 [21]
MgOH	− 164.8 ± 37.7 [9]; − 125 [19]; −92.1 ± 33.5 [20]
CaOH	− 193.9 ± 21.0 [9]; − 175.7 [19]
SrOH	− 205.5 ± 20.9 [9]; − 183 [19]
BaOH	− 266.4 ± 29.3 [9]; − 230 ± 17 [19]
$Ba(OH)_2$	− 626.6 ± 37.7 [9]; − 586 [19]

[a] References: JANAF Tables [9]; Lias et al. [19]; Operti et al. [20]; Huntelaar et al. [21].

5. Results and discussion

5.1. Ion formation reactions in flames

The H_2–O_2–N_2 flames contain only a small degree of natural ionization produced by the chemi-ionization reaction [23]

$$H + H + OH \rightleftarrows H_3O^+ + e^- \quad (8)$$

With H_3O^+; neutral metallic species can undergo chemical ionization (CI) by proton transfer

$$H_3O^+ + AO \rightleftarrows H_2O + AOH^+ \text{ or } AO.H^+ \quad (9)$$

$$H_3O^+ + AOH \rightleftarrows H_2O + AOH_2^+ \text{ or } A^+.H_2O \text{ or } AOH.H^+ \quad (10)$$

$$H_3O^+ + A(OH)_2 \rightleftarrows H_2O + A(OH)(H_2O)^+ \text{ or } AOH^+.H_2O \text{ or } A(OH)_2.H^+ \quad (11)$$

$$H_3O^+ + OAOH \rightleftarrows H_2O + A(OH)_2^+ \text{ or } AO^+.H_2O \text{ or } HOAO.H^+ \quad (12)$$

Metallic ions were also produced by chemi-ionization processes

$$AO + H \rightleftarrows AOH^+ + e^- \quad (13)$$

$$A + OH \rightleftarrows AOH^+ + e^- \quad (14)$$

$$OAOH + H \rightleftarrows A(OH)_2^+ + e^- \quad (15)$$

In each case, the back reaction represents electron-ion recombination. In general, the atomic A^+ ion is formed from, and linked to, the hydroxide AOH^+ ion by a fast balanced reaction

$$AOH^+ + H = A^+ + H_2O \quad (16)$$

Because $[H_2O]$ is large, it can be assumed that hydration reactions of ions are also rapid and balanced

$$A^+ + H_2O + M = A^+.H_2O + M \quad (17)$$

$$AOH^+ + H_2O + M = AOH^+.H_2O + M \quad (18)$$

$$A(OH)_2^+ + H_2O + M = A(OH)_2^+.H_2O + M \quad (19)$$

where M is a third body. When a pair of metallic compounds is introduced into a flame, a proton transfer reaction can occur

$$AOH^+ + A'O \rightleftarrows A'OH^+ + AO \quad (20)$$

The reactions of primary interest in the present work are the proton transfer reactions (9), (12), and (20); all three are examples of the general reaction (2). By adjusting the concentration of the salt solution in the atomizer, it was possible to achieve equilibrium for AOH^+ and $A'OH^+$ ions in all five fuel-rich flames.

5.2. Relaxation time τ

When the gas is sampled through the nozzle, it cools in two regions: in the thermal boundary layer surrounding the orifice; and in the near-adiabatic expansion downstream of the nozzle throat [24]. This can cause a shift of fast equilibrium reactions in the exothermic direction during sampling. In particular, the signals of ion hydrates which may not be genuine flame ions can be enhanced with respect to the parent ion signals. In general, if the relaxation time τ_2 of the proton transfer reaction (2) is greater than the sampling time of approximately 1 μs [24,25], it may be assumed that the reaction does not shift during sampling. Also, the equilibration of reaction (2) requires that the relaxation time $\tau_2 = 1/(k_2[B] + k_{-2}[X])$ is appreciably less than the time corresponding to 30 mm of flame represented by $\Delta z/v \approx 2$ ms, where v is the average rise velocity in the burnt gas of approximately 15 m s^{-1}. Thus, for a proton transfer reaction (2) to reach true equilibrium within the time scale of the flame without sampling distortion, the relaxation time τ_2 must fall into the time window 1 $\mu s < \tau_2 <$ 2 ms. Table 4 lists the relaxation times estimated for the reactions studied in this work. When A is an alkaline earth metal, a straightforward calculation in some cases yields a value of $\tau_2 > 10$ ms which is too large; it occurs when [AO] is a minor constituent, as shown in Table 2. Experimentally, however, profiles

Table 4
Estimated relaxation time τ_2 for reactions in flame 3 at $z = 30$ mm downstream

Reaction	τ_2 (ms)	τ_2 (μs)[a]
$SrOH^+ + BaO = BaOH^+ + SrO$	0.84	128
$CaOH^+ + BaO = BaOH^+ + CaO$	0.85	128
$CaOH^+ + SrO = SrOH^+ + CaO$	41.2	150
$SnOH^+ + CaO = CaOH^+ + SnO$	498	810
$H_3O^+ + CaO = CaOH^+ + H_2O$	400	137
$SnOH^+ + MgO = MgOH^+ + SnO$	14.7	532
$Y(OH)_2^+ + MgO = MgOH^+ + OYOH$	54.7	547
$H_3O^+ + MgO = MgOH^+ + H_2O$	10.8	272
$Y(OH)_2^+ + SnO = SnOH^+ + OYOH$	0.12	···
$H_3O^+ + SnO = SnOH^+ + H_2O$	0.10	···
$H_3O^+ + OYOH = Y(OH)_2^+ + H_2O$[b]	1×10^{-5}	···

[a] Additional proton transfer to $A(OH)_2$ is included.
[b] The reaction will shift because of sampling cooling.

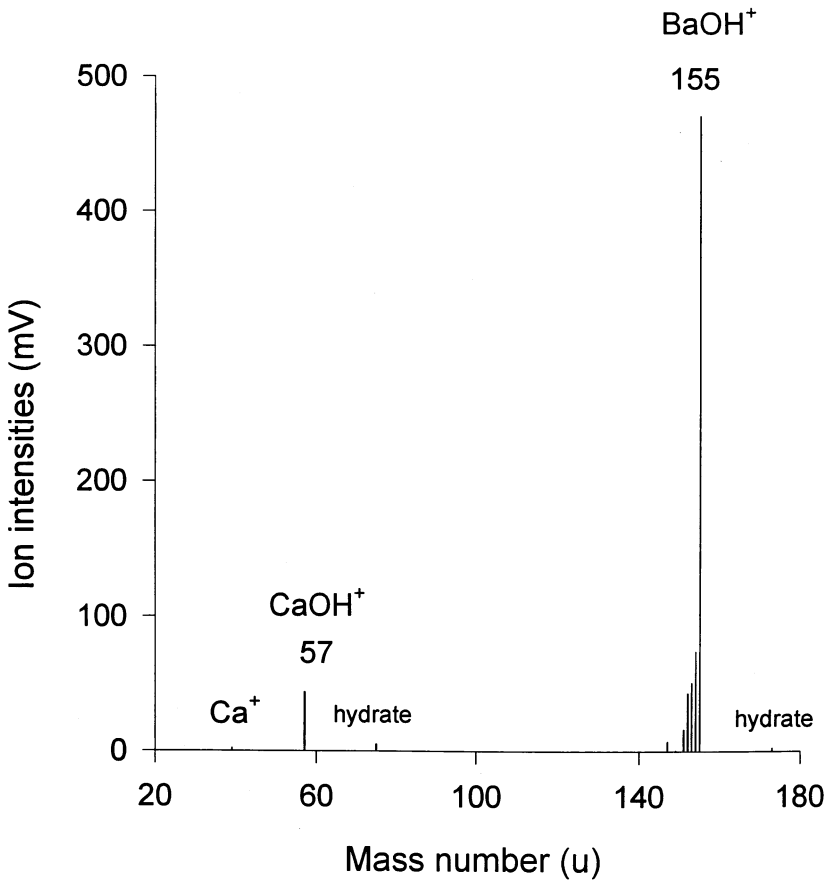

Fig. 2. Mass spectrum at high resolution measured downstream at $z = 30$ mm in flame 2 with the atomizer spraying a mixed solution of 0.1 M $CaAc_2$ and 0.01 M $BaCl_2$.

of these ions often achieve constant plateau values indicative of equilibrium for $z < 30$ mm (i.e. 2 ms). The answer lies in the fact that there is another route to form AOH^+ involving proton transfer by H_3O^+ to the major constituent $A(OH)_2$ via reaction (11) followed by rapid dissociation of the $A(OH)(H_2O)^+$ product ion to give AOH^+ via reaction (− 18). The inclusion of $[A(OH)_2]$ from Table 4 into the expression for τ_2 yields a value which falls into the time window such that the assumption of equilibrium is warranted. For this estimate, a value of $k_2 = 5 \times 10^{-9}$ cm^3 $molecule^{-1}$ s^{-1} was assumed for normal flame temperatures of about 2100 K, with k_{-2} reduced by an exponential factor corresponding to the endothermicity of the back reaction.

5.3. Experimental results for alkaline earth metals

Fig. 2 shows the mass spectrum of a mixture containing 0.1 M $CaAc_2$ and 0.01 M $BaCl_2$ in flame 2 at $z = 30$ mm downstream. The two most intense peaks are because of $^{40}CaOH^+$ at 57 u and $^{138}BaOH^+$ at 155 u. Barium has five major isotopes which can be seen clearly in the mass spectrum. The very small peaks at 40, 75, and 173 u arise from Ca^+, $CaOH^+.H_2O$, and $BaOH^+.H_2O$, respectively. The hydrate ion signals increase noticeably for the low-temperature flames, and they are not considered to be genuine flame ions [26]. Fig. 3 shows the time-resolved profiles for the ions of Fig. 2. All of the ion signals, including the total positive ion (TPI) profile, reach constant plateau values down-

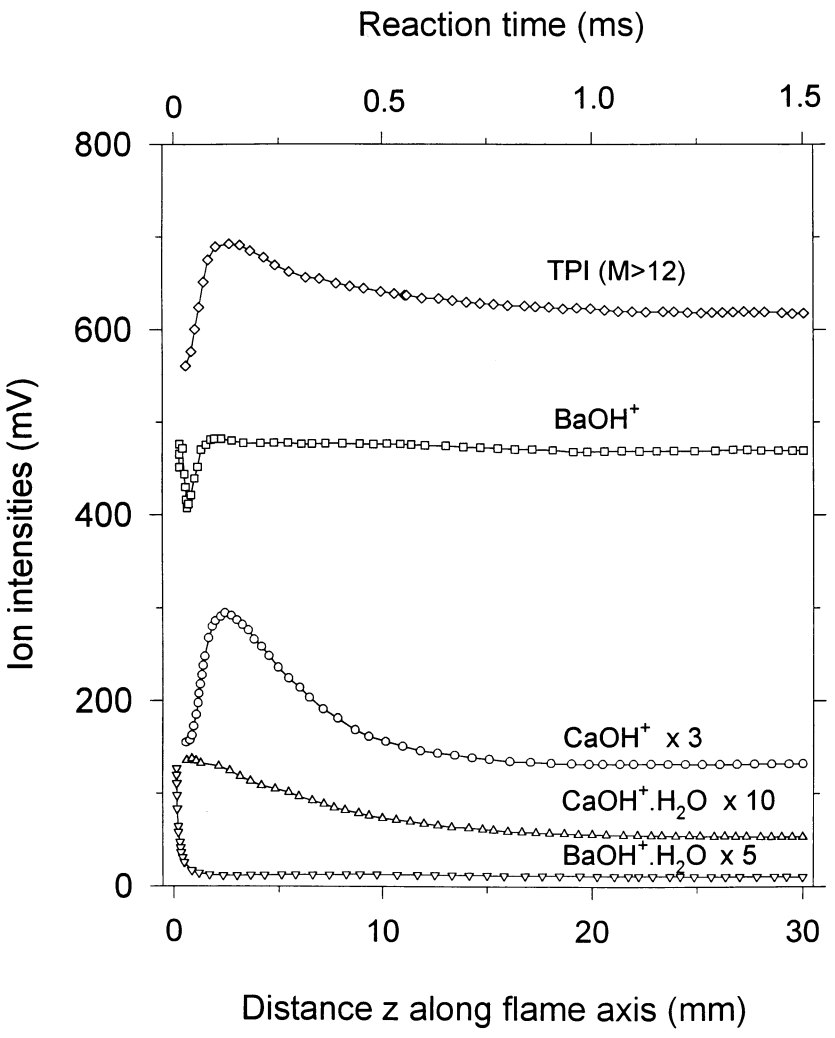

Fig. 3. Ion profiles measured at low resolution in flame 2 of concentration vs axial distance z or reaction time, with the atomizer spraying a mixed solution of 0.1 M $CaAc_2$ and 0.01 M $BaCl_2$; TPI_{12} denotes total positive ions. The flame reaction zone is located near $z = 0$ mm.

stream of $z \geq 15$ mm (0.75 ms), and yield a constant equilibrium ratio $[BaOH^+]/[CaOH^+]$; the hydrate signals were added to the parent ion signals in calculating the ion ratio. The two ions $BaOH^+$ and $CaOH^+$ are related by reaction (20) for proton transfer between CaO and BaO whose reaction enthalpy $\Delta H^0_{20} = PA^0(CaO) - PA^0(BaO)$, the difference of their proton affinities. The equilibrium constant for reaction (20) was then calculated from the constant ratio of the ion currents and the known concentration ratio of the neutral reactants (Table 2) at $z = 30$ mm, where $K_{20} = ([BaOH^+]/[CaOH^+])([CaO]/[BaO])$ in this case. The oxide concentration [AO] is a function of γ [18] so that values of γ at $z = 30$ mm were included in [CaO]/[BaO] where appropriate.

A van't Hoff plot of ln K_{20} vs $1/T$ for the five fuel-rich flames covering the temperature range 1820–2400 K is given in Fig. 4. A least-squares fit through the data points yields a reasonably good straight line, although there is noticeable curvature. The three sets of points were obtained from different experiments employing different sample concentra-

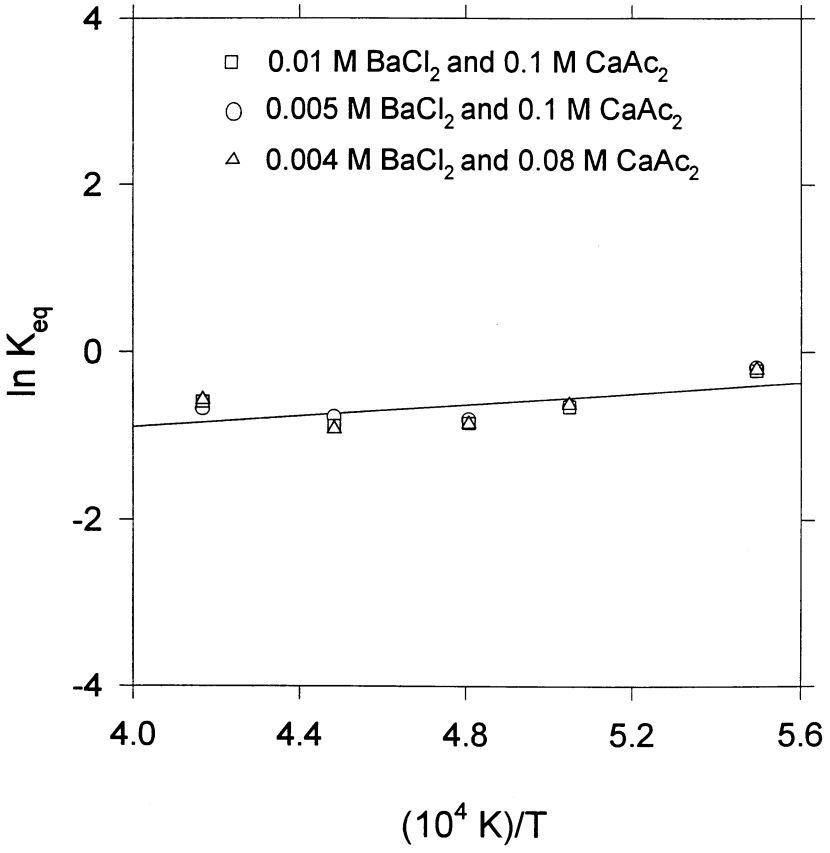

Fig. 4. Van't Hoff plot for the equilibrium constant of the proton transfer reaction (20) involving $BaOH^+$ and $CaOH^+$ measured in five flames over the temperature range 1820–2400 K with the atomizer spraying mixed aqueous solutions of varying concentrations and Ba/Ca ratios as indicated.

tions and ratios for the $BaCl_2/CaAc_2$ mixed solution, with a sampling nozzle diameter of 0.170 mm. From the slope $\Delta H^0 = -28.0 \pm 9.2$ kJ mol^{-1} (-6.7 ± 2.2 kcal mol^{-1}), and from the intercept $\Delta S^0 = -18.8 \pm 4.6$ J mol^{-1} K^{-1} (4.5 ± 1.1 cal mol^{-1} K^{-1}). The error limit reported here represents the standard deviation of the least-squares fit, and the plot shows that the experimental data are consistent and reproducible. Theoretically speaking, $\Delta S^0 \approx 0$ for a simple proton transfer like reaction (20). The major contribution to this rather large ΔS^0 value might have arisen from mass discrimination and/or the hydrate contributions of AOH^+. As discussed above, these effects can modify the intercept but not the value of ΔH^0 derived from the slope. This important consideration lends credibility to the PA values obtained.

Another example is the proton transfer reaction between SrO and BaO. A van't Hoff plot is shown in Fig. 5. In this case, three different orifice diameters (0.104, 0.170 mm Pt/Ir and 0.181 mm Ni) were used with the atomizer spraying a solution of 0.1 M $SrAc_2$ and 0.025 M $BaCl_2$. Here, $\Delta H^0 = -10.9 \pm 8.8$ kJ mol^{-1} (-2.6 ± 2.1 kcal mol^{-1}), and $\Delta S^0 = -13.8 \pm 5.9$ J mol^{-1} K^{-1} (-3.3 ± 1.4 cal mol^{-1} K^{-1}). A similar van't Hoff plot (not shown) for the proton transfer reaction between CaO and SrO yields $\Delta H^0 = -17.2 \pm 10.0$ kJ mol^{-1}, and $\Delta S^0 = -6.7 \pm 5.4$ J mol^{-1} K^{-1}. These experimental results show that $PA^0(BaO) > PA^0(SrO) > PA^0(CaO)$, in agreement with Murad's values [7] but in contrast to those derived from the JANAF Tables [9]. This is primarily because of the different values of the ionization energy of BaOH

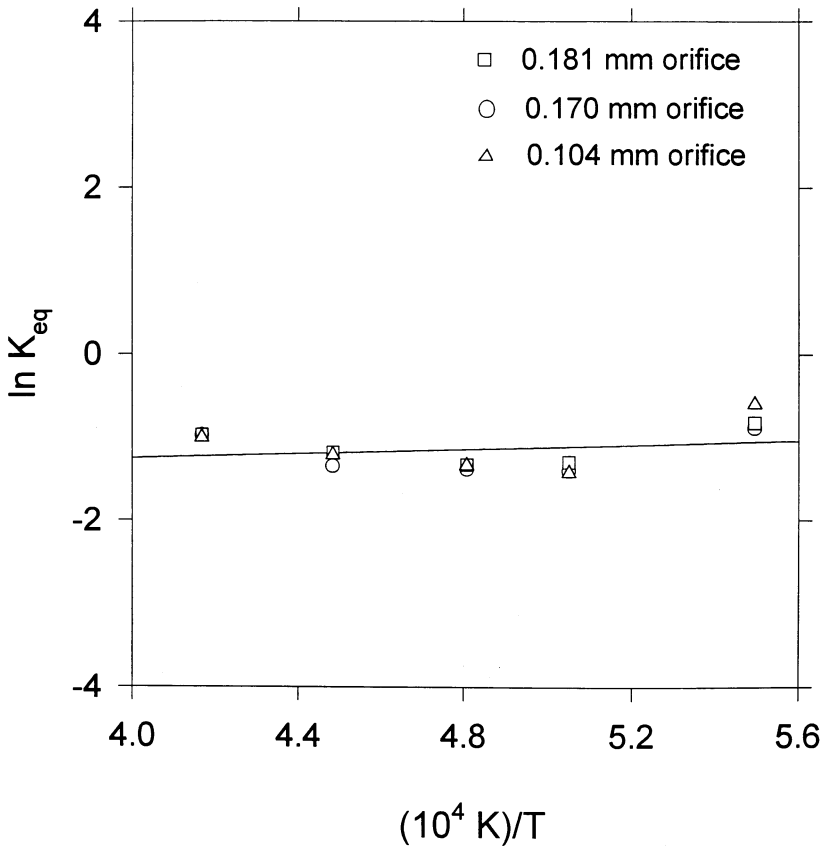

Fig. 5. Van't Hoff plot for the equilibrium constant of the proton transfer reaction (20) involving $BaOH^+$ and $SrOH^+$ measured in five flames over the temperature range 1820–2400 K. The atomizer was spraying a mixed aqueous solution of 0.025 M $BaCl_2$ and 0.1 M $SrAc_2$ for different sampling nozzles of varying diameter as indicated.

quoted by different authors. In the JANAF Tables, $IE^0(BaOH) = 5.09$ eV which is the average of two separate measurements [27,28]. The most recent literature reference gives the value as 4.62 ± 0.3 eV [26]. Murad measured $IE^0(BaOH) = 4.35 \pm 0.3$ eV [7]; from $IE^0(BaOH) = \Delta H_f^0(BaOH)^+) - \Delta H_f^0(BaOH)$ and $\Delta H_f^0(BaOH) = -230 \pm 18$ kJ mol^{-1} (the JANAF Tables give a value of -222 ± 29 kJ mol^{-1}), he obtained $\Delta H_f^0(BaOH^+) = 189$ kJ mol^{-1}. Thus, he arrived at a value for $PA^0(BaO) = \Delta H_f^0(BaO) + \Delta H_f^0(H^+) - \Delta H_f^0(BaOH^+) = 1216$ kJ mol^{-1} (291 kcal mol^{-1}) which is 70 kJ mol^{-1} (17 kcal mol^{-1}) higher than the value of 1146 kJ mol^{-1} (274 kcal mol^{-1}) derivable from the JANAF Tables [9].

Generally speaking, an equilibrium constant such as K_{20} must be independent of both the size of the orifice and the concentration ratio of the metals in the salt solution. A change in the latter ratio by a factor of 2–5 at a given temperature was possible for some samples. This is small compared with HPMS experiments, where the neutral concentration ratio can be varied by a factor of more than 10. The restriction occurs in FIMS because the ratio of metallic neutrals is fixed in a given flame (see Table 2) and, when considerations of the relaxation time are included (see Sec. 5.2), there is relatively little room to alter the concentration ratio in the salt solution.

5.4. Proton affinity ladder

Similar to the alkaline earth metals, experiments were also conducted for the pairs CaO/SnO, CaO/

Table 5
Results from slopes and intercepts of the van't Hoff plots

Reaction	$-\Delta H^0$ (kJ mol^{-1})	$-\Delta S^0$ (J mol^{-1} K^{-1})
$SrOH^+ + BaO = BaOH^+ + SrO$	10.9 ± 8.8	13.8 ± 5.9
$CaOH^+ + BaO = BaOH^+ + CaO$	28.0 ± 9.2	18.8 ± 4.6
$CaOH^+ + SrO = SrOH^+ + CaO$	17.2 ± 10.0	6.7 ± 5.4
$SnOH^+ + CaO = CaOH^+ + SnO$	268.0 ± 15.0	9.4 ±7.2
$H_3O^+ + CaO = CaOH^+ + H_2O$	492.5 ± 81.7[a]	− 31.7 ± 35.4[a]
$SnOH^+ + MgO = MgOH^+ + SnO$	99.2 ± 8.8	13.4 ± 3.8
$Y(OH)_2^+ + MgO = MgOH^+ + OYOH$	245.6 ± 16.9	83.5 ± 7.5
$H_3O^+ + MgO = MgOH^+ + H_2O$	324.9 ± 8.8	− 4.5 ± 4.3
$Y(OH)_2^+ + SnO = SnOH^+ + OYOH$	153.5 ± 17.6	69.8 ± 8.5
$H_3O^+ + SnO = SnOH^+ + H_2O$	218.0 ± 10.5	− 15.9 ± 5.0

[a] K_{eq} was measured only at temperatures of 2230 (flame 25) and 2400 K (flame 2).

H_2O, MgO/SnO, MgO/OYOH, SnO/OYOH, MgO/H_2O, and SnO/H_2O. The results of ΔH^0 and ΔS^0 derived from van't Hoff plots for each individual pair of compounds are given in Table 5. In order to set up a PA ladder, selecting a suitable reference base B is very important for the measurement of the unknown proton affinity of a molecule X. Consider the general reaction (2). If $PA^0(B)$ is considerably higher than $PA^0(X)$, i.e. the reaction is exothermic to the right, then $K_{eq} = k_2/k_{-2}$ is very large so that $k_2 \gg k_{-2}$ for the forward and back reactions. In order to obtain the value of K_{eq}, the neutral concentration ratio [X]/[B] must be very large if the ratio of the ion currents is to be in a range suitable for measurement. Using SnO/H_2O as an example, the major flame product is water with $[H_2O] \approx 1 \times 10^{18}$ molecule cm^{-3} at 2100 K; at the same temperature, the tin oxide concentration in flame 3 is $[SnO] \approx 3 \times 10^{12}$ molecule cm^{-3}. Therefore, even though the proton transfer reaction from H_3O^+ to SnO is strongly exothermic ($PA^0(SnO) - PA^0(H_2O) \approx 215$ kJ mol^{-1} = 52 kcal mol^{-1}), H_2O in the role of an anchor can still be used as a reference base to obtain the PA values for metallic oxides. This is valid because the large concentration ratio $[H_2O]/[SnO] \approx 3 \times 10^5$ brings H_3O^+ and $SnOH^+$ ions into equilibrium in flames [29]. The large amount of water present here is also a crucial factor in forcing H_3O^+ and $MgOH^+$, and even $CaOH^+$, to overcome the endothermicity of the reverse reaction so that equilibrium is attained. With these considerations in mind, the PA ladder presented in Fig. 6 was constructed.

The exothermicity gap for CaO/H_2O is so large that the attainment of equilibrium stretches the method to the limit. With the atomizer spraying 0.004 M $CaAc_2$, $[H_2O]/[CaO] \approx 7 \times 10^9$ at 2400 K in flame 2 and K_{eq} could be measured only for the two highest-temperature flames, 2 and 25. The two-point van't Hoff plot (not shown) yields $\Delta H^0 = -492.5 \pm 81.7$ kJ mol^{-1} (-117.7 ± 19.5 kcal mol^{-1}), and $\Delta S^0 = 31.7 \pm 35.4$ J mol^{-1} K^{-1} (7.6 ± 8.5 cal mol^{-1} K^{-1}); the high uncertainties stem from a number of measurements which were not very consistent. The large experimental value obtained for ΔS^0 with its large uncertainty is not inconsistent with the value of 15.7 J mol^{-1} K^{-1} derived from the JANAF Tables [9] at 2100 K. For the other low-temperature flames 3–5, the H_3O^+ ion signal was too small to be measured. In order to boost the H_3O^+ ion signal, an even lower concentration of $CaAc_2$ solution was attempted, but the problem was complicated by the requirement of the relaxation time. In this case, although the H_3O^+ ion signal was measurable, H_3O^+ and $CaOH^+$ did not reach equilibrium in the time window available for the flame. Because of the large uncertainties of the ΔH^0 and ΔS^0 values, the measurement cannot be taken too seriously; hence, only a dashed line is used as an indicator to link H_2O and CaO in the PA ladder given in Fig. 6.

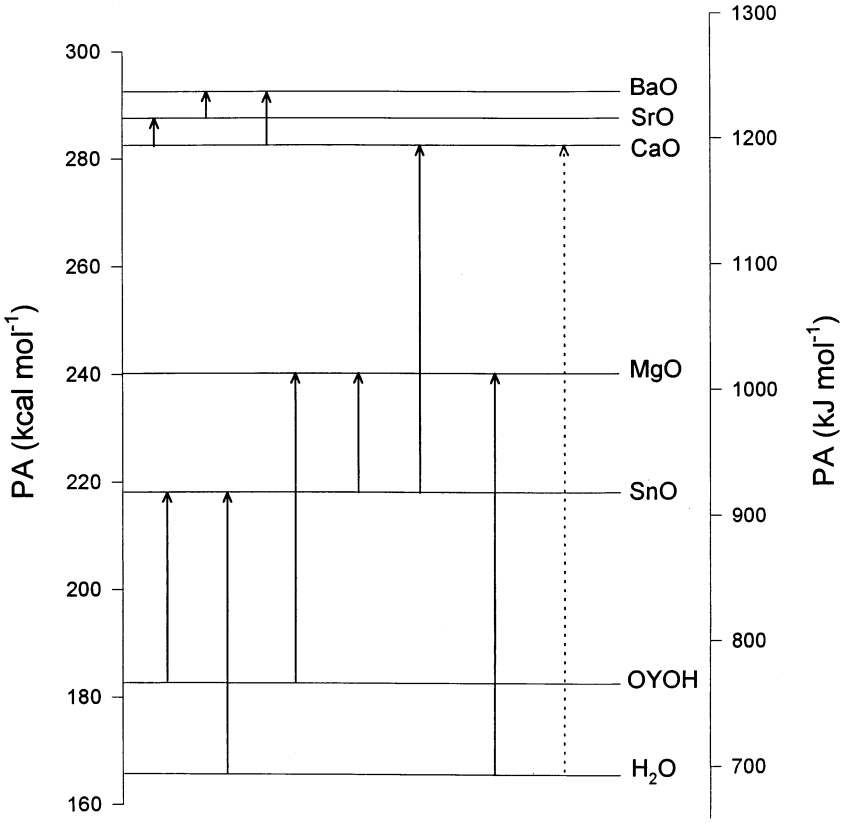

Fig. 6. Proton affinity ladder for metallic compounds involving equilibrium measurements of pairs of ions related to the neutral species indicated by the arrows.

By similar reasoning, if the ions of a pair of metallic compounds reach equilibrium, the neutral concentration of the molecule of lower PA in the flame must exceed that of the molecule of higher PA; in general, the same must be true for the concentrations of the metallic salts in the atomizer. For example, the proton transfer reaction between $CaOH^+$ and $SnOH^+$ can reach equilibrium during the time window of the flame because the [SnO]/[CaO] ratio is very large. Ion profiles for this equilibrium reaction measured in flame 2 are shown in Fig. 7. In contrast, both [MgO] and [CaO] are minor species and the equilibrium between $MgOH^+$ and $CaOH^+$ cannot be achieved within the time window available for FIMS. Therefore, the link reaction between the top and the bottom of the PA ladder is the proton transfer reaction involving $CaOH^+/SnOH^+$ instead of $CaOH^+/MgOH^+$. From the van't Hoff plot for CaO/SnO shown in Fig. 8, $\Delta H^0 = -268.0 \pm 15.0$ kJ mol^{-1} (-64.1 ± 3.6 kcal mol^{-1}), and $\Delta S^0 = -9.4 \pm 7.2$ J mol^{-1} K^{-1} (-2.2 ± 1.7 cal mol^{-1} K^{-1}). Because PA^0(SnO) has been determined with reference to water [29] and has also been calculated theoretically by ab initio methods [30], SnO can serve as another firm anchor, i.e. an alternative reference base to water. In addition, it is helpful that [SnO] $\approx$ 100% of the tin present in flames.

Thermodynamic values for the neutral species of the group 3 metals scandium, yttrium, and lanthanum are not available in the JANAF Tables [9]. Previous work in this laboratory indicated that only YO and OYOH exist in flames, and their neutral concentrations were estimated [31]. The $Y(OH)_2^+$ ion was observed in the mass spectrum but not YOH^+. Ex-

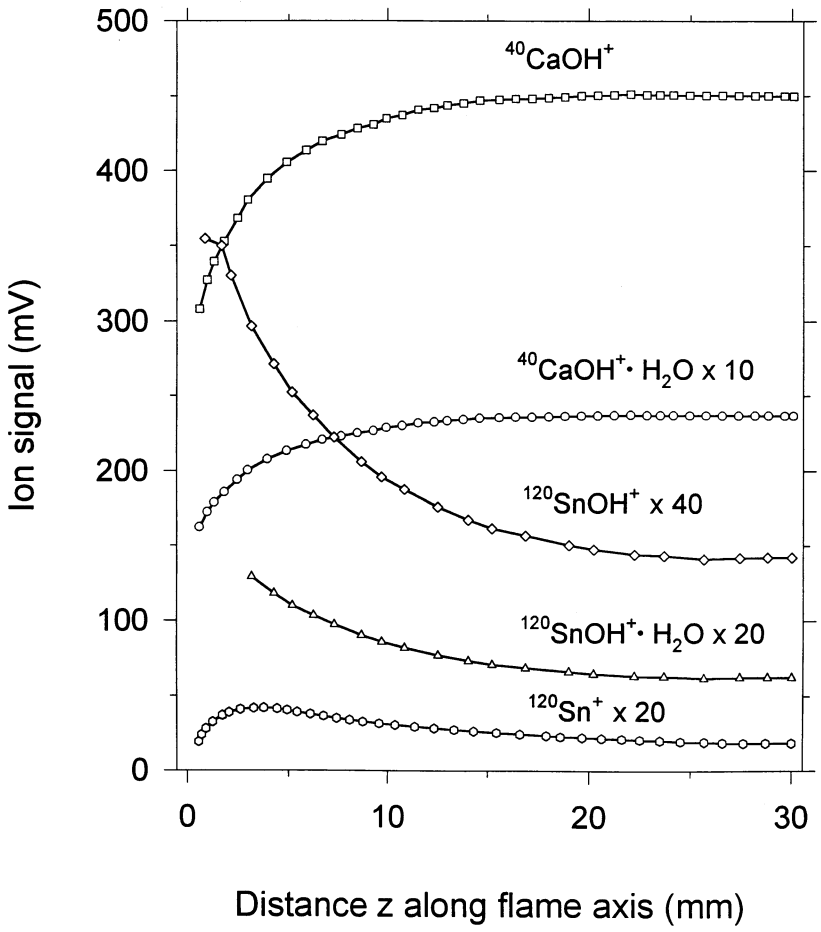

Fig. 7. Ion profiles measured at high resolution in flame 2 with the atomizer spraying a mixed solution of 0.092 M $SnCl_4$ and 0.008 M $CaAc_2$. The flame reaction zone is located near $z = 0$ mm.

periments were carried out to obtain PA^0(OYOH) using SnO as a reference base. From the van't Hoff plot shown in Fig. 9, $\Delta H^0 = -153.5 \pm 17.6$ kJ mol^{-1} (-36.7 ± 4.2 kcal mol^{-1}), and $\Delta S^0 = -69.8 \pm 8.5$ J mol^{-1} K^{-1} (-16.7 ± 2.0 cal mol^{-1} K^{-1}). The reason for the large ΔS^0 value is not clear at this time, but estimates from isoelectronic neutral species indicate that a rather large value is reasonable. The ΔH^0 value from Fig. 9 gives PA^0(OYOH) = 765.7 kJ mol^{-1} (183 kcal mol^{-1}); compared to the PAs of the metallic oxides, the PA value for OYOH seems low.

Another experiment was also attempted to measure PA^0(OYOH) using water as a reference base. However, the relaxation time $\tau < 1$ μs causing the proton transfer reaction between H_3O^+ and $Y(OH)_2^+$ to shift in the exothermic direction because of sampling cooling so that H_3O^+ became too small to be measured. In an attempt to boost the ionization level, 0.25 mol% of methane was added to the flame to raise $[H_3O^+]$ but the ion profiles did not reach constant plateau values downstream. That is, equilibrium between H_3O^+ and $Y(OH)_2^+$ could not be achieved within the time scale of the flame, and water cannot be used as a reference base in this case. Nevertheless, if thermodynamic data for the neutral species of the group 3 metals become available, future work can yield PA values for OLaOH and OScOH.

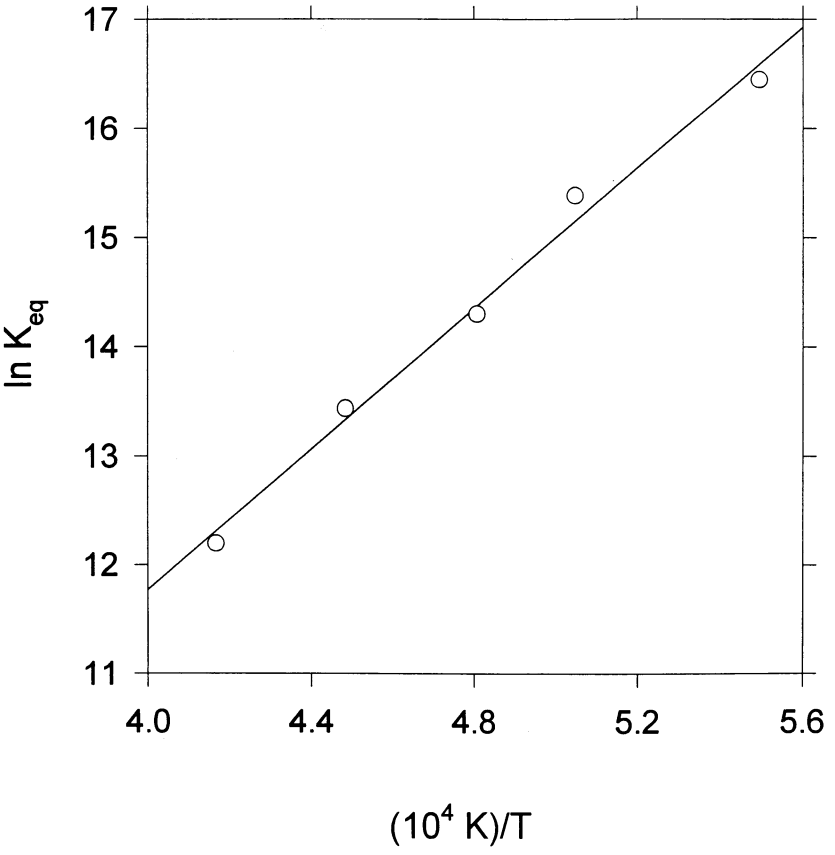

Fig. 8. Van't Hoff plot for the equilibrium constant of the proton transfer reaction (20) involving $CaOH^+$ and $SnOH^+$ measured in five flames over the temperature range 1820–2400 K with the atomizer spraying mixed aqueous solutions of $SnCl_4$ and $CaAc_2$.

5.5. Correction of PA values from flame to room temperature

All the measurements were made at flame temperatures in the range 1820–2400 K with an average value very close to 2100 K corresponding to the midpoint of the van't Hoff plots. By convention, PA values are quoted at 298 K requiring the correction of the flame data to room temperature. For the alkaline earth metals according to the JANAF Tables [9], $PA^0_{2100}(AO) - PA^0_{298}(AO) = 25.442$, 10.242, 9.387 and 4.867 kJ mol^{-1} for A = Mg, Ca, Sr and Ba, respectively, and the PA difference for H_2O is 13.285 kJ mol^{-1}; data for SnO and OYOH are not listed. In general, the PA difference between flame and room temperature is $\leq$ 14 kJ mol^{-1} ($\leq$ 3.5 kcal mol^{-1}); MgO is an exception. Using $PA^0(H_2O)$ = 691.0 kJ mol^{-1} (165.2 kcal mol^{-1}) [1] as an anchor, the corrected PA values at 298 K are listed in Table 6 in both kJ and kcal mol^{-1}. Based on the references cited here, a reasonable assessment of the errors for the PA values listed in Table 6 is $\pm$ 21 kJ mol^{-1} ($\pm$ 5 kcal mol^{-1}).

The value of $PA^0(MgO) = 1004 \pm 21$ kJ mol^{-1} at 298 K is based on thermodynamic data in the JANAF Tables [9] for neutral Mg, MgO, MgOH, and $Mg(OH)_2$, some of which are controversial. Other values in the literature for $PA^0(MgO)$ are higher than Murad's value of 988 kJ mol^{-1} [7] quoted in the NIST compilation [1]. Our recent theoretical and experimental study of magnesium [22] (see Sec. 4) yields a calculated value of 1078 $\pm$ 13 and an exper-

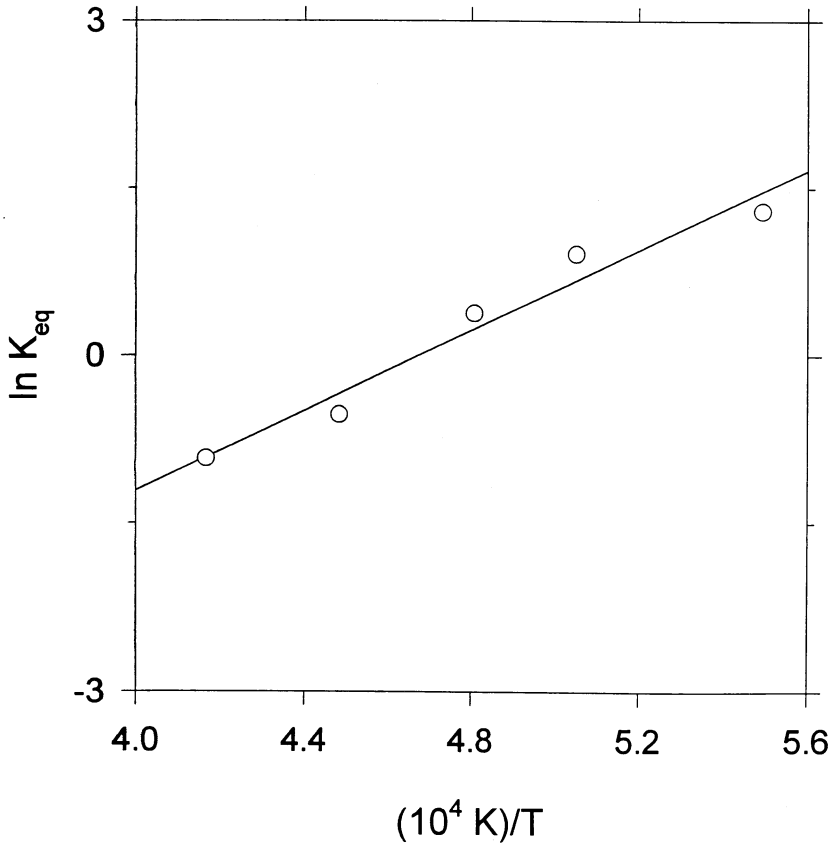

Fig. 9. Van't Hoff plot for the equilibrium constant of the proton transfer reaction (20) involving $SnOH^+$ and $Y(OH)_2^+$ measured in five flames over the temperature range 1820–2400 K with the atomizer spraying mixed aqueous solutions of $SnCl_4$ and YCl_3.

imental one of 1056 ± 29 kJ mol^{-1} in good agreement. These results are also in good agreement with the higher value of 1071 ± 29 kJ mol^{-1} determined by Operti et al. [20].

5.6. Proton transfer linking alkali and alkaline earth metals

It would be of interest to investigate proton transfer between compounds of alkali and alkaline earth metals. PA values for alkali metal hydroxides have been well established by Kebarle and his coworkers [4,5]. A promising pair of such metal compounds for FIMS is LiOH/SrO with proton transfer involving the ions $LiOH_2^+$ and $SrOH^+$. Our experimental attempts with this system to date have not been successful. $PA^0(LiOH) = 1007$ kJ mol^{-1} (240.7 kcal mol^{-1}) [4] is an ideal reference base to link the low and high ends of the PA ladder. Unlike the other alkali metals, neutral LiOH is a major species in flames with [LiOH] ≥ 90%; the only other species is atomic Li. The mass spectrum of lithium is different from that of the other alkali metals. Because $IE^0(Li) = 5.392$ eV is small, the thermal ionization of lithium is the important production reaction, and atomic Li^+ is the major peak

$$Li + M = Li^+ + e^- + M \quad (21)$$

At the same time, $LiOH_2^+$ ($= Li^+.H_2O = LiOH\,.\,H^+$) yields a relatively small peak. The measurement of the proton transfer product $LiOH_2^+$

Table 6
Proton affinities of metallic compounds at 298 K

Compound	Proton affinity				
	Literature value			This work	
	kJ mol^{-1}	kcal mol^{-1}	Author [Ref.]	kJ mol^{-1}	kcal mol^{-1}
BaO	1215	291	Murad [7]	1222	292
SrO	1209	289	Murad [7,8]	1201	287
CaO	1191	285	Murad [7,8]	1184	283
CsOH	1126	269.2	Kebarle [5]		
KOH	1099	262.6	Kebarle [5]		
NaOH	1036	247.6	Kebarle [5]		
LiOH	1007	240.7	Kebarle [5]		
MgO	988	236	Murad [7]	1004	240
FeO	918	219	Murad [3]		
SnO	899	215	Jensen [12]	912	218
CuOH	891	213	Hayhurst [10]		
OYOH				766	183
H_2O	691.0	165.2	NIST [1]		

$$LiOH + SrOH^+ = LiOH_2^+ + SrO \quad (22)$$

was complicated by extensive hydration of the Li^+ ion by the cooling which occurs during sampling

$$Li^+ + H_2O + M = Li^+.H_2O + M \quad (23)$$

In this case, only a small part of the $LiOH_2^+$ observed in the mass spectrum come from the genuine flame ion and most of it was hydrate formed during sampling. Hence, instead of measuring the ion intensity of $LiOH_2^+$, Li^+ ion intensities were measured. Under the assumption that ΔH^0 and ΔS^0 for reaction (23) do not change from 298 K to flame temperature, and using data from the work of Kebarle and his co-workers [5], the genuine ratio $[LiOH_2^+]/[Li^+]$ was calculated at flame temperatures. The calculations indicated that over 98% of the measured $LiOH_2^+$ ion signal was formed by hydration and the contribution of the genuine flame ion was very small. Significantly, the calculated $[LiOH_2^+]$ concentrations did not yield the correct ΔH^0 value for reaction (22). Also, it was difficult to bring Sr and Li ions into equilibrium within the time window of the flame. Thus, a number of the problems encountered were formidable, and the alkali metals were not pursued further at this time.

6. Summary

These quantitative measurements of ion-molecule equilibria at 760 Torr and flame temperatures by the FIMS method led to the successful construction of a proton affinity ladder with high PA values for metallic compounds which include alkaline earth oxides, tin oxide, and yttrium oxide-hydroxide. With H_3O^+, a natural flame ion, to anchor this ladder to $PA^0(H_2O)$, a new PA value for OYOH was measured. In general, the PA values obtained here for the alkaline earths are in excellent agreement with previous measurements done by Murad which are listed in the NIST compilation (see Table 6). This new approach using FIMS to obtain PA values of metallic compounds has some distinct advantages. The relative PA values are not subject to mass discrimination. Metallic species can be observed in flames which are not accessible at lower temperatures. The proton transfer equilibria can be measured over a considerable range of high temperatures. Because a thermodynamic measurement is involved, the flame rise velocity in the burnt gas is not an important parameter (it is crucial for kinetic measurements). An even larger temperature range is available for such measurements (say, 1700–2550 K, not limited to the range of flames 2–5) and any

temperature in between. Using water as an anchor reference base, $\Delta PA^0 > 210$ kJ mol^{-1} (50 kcal mol^{-1}), or even up to 490 kJ mol^{-1} (117 kcal mol^{-1}), can be bridged between water and metallic oxides (e.g. SnO, MgO, and even CaO) to build the PA ladder. At the same time, FIMS has some shortcomings. Unlike HPMS, neutral concentrations of metallic species at flame temperatures are calculated and not directly measured. Current thermodynamic data for metallic compounds from different literature sources are sometimes in conflict (see Table 3), and are often not available, e.g. transition metals. Also, it can be difficult to bring a pair of ions into equilibrium in the time scale of the flame imposed by the relaxation time τ and sampling considerations.

In future studies, when accurate thermodynamic data become available for other neutral metallic species, FIMS offers the opportunity for the measurement of PA values for a considerable range of such compounds at the high end of the PA scale. Some of these compounds are also accessible by KCMS. These studies compliment those lower down on the PA scale which have produced so many values for organic compounds by the FA (SIFT), HPMS and ICR methods.

Acknowledgements

Support of this work by the Natural Sciences and Engineering Research Council (NSERC) of Canada is gratefully acknowledged.

References

[1] E.P. Hunter, S.G. Lias, Proton Affinity, NIST Chemistry WebBook, NIST Standard Reference Database Number 69—March 1998 Release (http://webbook.nist.gov/chemistry/paser.htm).
[2] S.G. Lias, J.F. Liebman, R.D. Levin, J. Phys. Chem. Ref. Data 13 (1984) 695, with subsequent additions and corrections.
[3] P.M. Hierl, J.F. Friedman, T.M. Miller, I. Dotan, M. Menendez-Barreto, J.V. Seeley, J.S. Williamson, F. Dale, P.L. Mundis, R.A. Morris, J.F. Paulson, A.A. Viggiano, Rev. Sci. Instrum. 67 (1996) 2142.
[4] S.K. Searles, I. Džidić, P. Kebarle, J. Am. Chem. Soc. 91 (1969) 2810.
[5] I. Džidić, P. Kebarle, J. Phys. Chem. 74 (1970) 1466.
[6] E. Murad, J. Chem. Phys. 73 (1980) 1381.
[7] E. Murad, J. Chem. Phys. 75 (1981) 4080.
[8] E. Murad, J. Chem. Phys. 78 (1983) 6611.
[9] M.W. Chase, Jr., C.A. Davies, J.R. Downey Jr., D.J. Frurip, R.A. McDonald, A.N. Syverud, J. Phys. Chem. Ref. Data 14 (1985) (Suppl. 1).
[10] C.J. Butler, A.N. Hayhurst, J. Chem. Soc., Faraday Trans. 93 (1997) 1497.
[11] D.E. Jensen, J. Chem. Phys. 51 (1969) 4675.
[12] R. Colin, J. Drowart, G. Verhaegen, Trans. Faraday Soc. 61 (1965) 1364.
[13] A.N. Hayhurst, D.B. Kittelson, Proc. R. Soc. London, Ser. A. 338 (1974) 155.
[14] J.M. Goodings, C.S. Hassanali, P.M. Patterson, C. Chow, Int. J. Mass Spectrom. Ion Processes 132 (1994) 83.
[15] J.M. Goodings, S.M. Graham, W.J. Megaw, J. Aerosol Sci. 14 (1983) 679.
[16] J.E. Szulejko, T.B. McMahon, J. Am. Chem. Soc. 115 (1993) 7839.
[17] C.E. Allison, T.B. McMahon, J. Am. Chem. Soc. 112 (1990) 1672.
[18] A.N. Hayhurst, D.B. Kittelson, Proc. R. Soc. London, Ser. A. 338 (1974) 175.
[19] S.G. Lias, J.F. Liebman, J.L. Holmes, R.D. Levin, W.G. Mallard, J. Phys. Chem. Ref. Data 17 (1988) (Suppl. 1).
[20] L. Operti, E.C. Tews, T.J. MacMahon, B.S. Freiser, J. Am. Chem. Soc. 111 (1989) 9152.
[21] M.E. Huntelaar, E.H.P. Cordfunke, J. Chem. Thermodynamics 29 (1997) 817.
[22] Q.F. Chen, R.K. Milburn, A.C. Hopkinson, D.K. Bohme, J.M. Goodings, Int. J. Mass Spectrom., to be published.
[23] S.D.T. Axford, A.N. Hayhurst, J. Chem. Soc., Faraday Trans. 91 (1995) 827.
[24] A.N. Hayhurst, D.B. Kittelson, Combust. Flame 28 (1977) 137.
[25] A.N. Hayhurst, N.R. Telford, Proc. R. Soc. London, Ser. A 322 (1971) 483.
[26] J.M. Goodings, P.M. Patterson, A.N. Hayhurst, J. Chem. Soc. Faraday Trans. 15 (1995) 2257.
[27] R. Kelly, P.J. Padley, Trans. Faraday Soc. 67 (1971) 1384.
[28] D.E. Jensen, Combustion and Flame 12 (1968) 261.
[29] J.M. Goodings, Q.F. Chen, Can. J. Chem. (in press).
[30] C.F. Rodriquez, A. Cunje, A.C. Hopkinson, J. Mol. Structure (Theochem) 430 (1998) 149.
[31] Q.F. Chen, J.M. Goodings, Int. J. Mass Spectrom. Ion Processes 176 (1998) 1.